

Supplementary Information

Tuning Ferrous Coordination Structure Enables a Highly Reversible Fe Anode for Long-life All-iron Flow Batteries

Yuxi Song,^{a,b} Kaiyue Zhang,^a Xiangrong Li,^a Chuanwei Yan,^a Qinghua Liu,^{c*} Ao Tang,^{a*}

^a Institute of Metal Research, Chinese Academy of Sciences, Shenyang, China

^b School of Material Science and Engineering, University of Science and Technology of China, Shenyang, China.

^c National Institute of Clean-and-Low-Carbon Energy, Beijing, China

*Corresponding author:

Ao Tang Email: a.tang@imr.ac.cn

Qinghua Liu Email: liuqinghua@chnenergy.com.cn

Tel: +86-024-81083919 Fax: +86-024-23998320

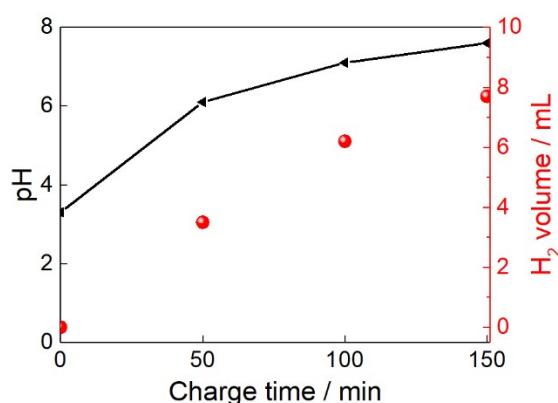


Fig. S1. The relationship between pH variation and H₂ evolution during charging.
Note: Measurements of pH and H₂ collection were taken in a three-electrode system.

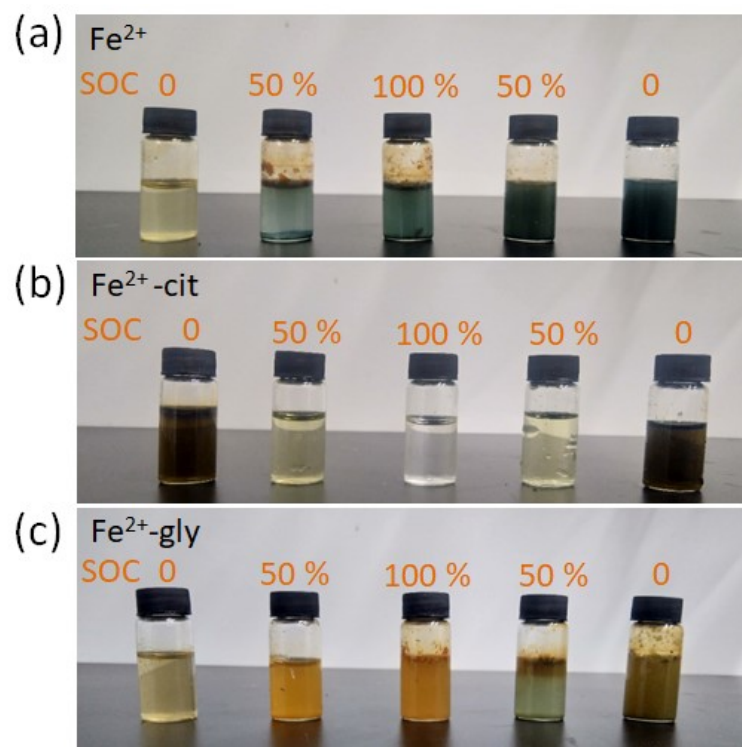


Fig. S2. The photos of (a) FeCl_2 , (b) Fe^{2+} -cit and (c) Fe^{2+} -gly at different SOCs in the charge-discharge tests.

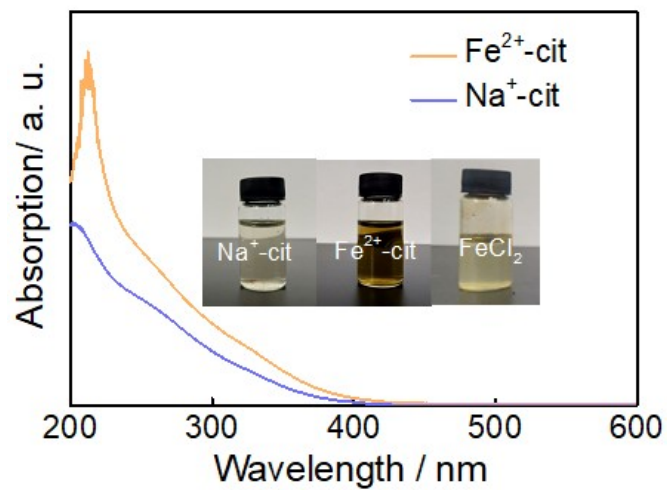


Fig. S3. The UV-vis spectrum of Fe²⁺-cit and Na⁺-cit. Inset: photos of Na⁺-cit, Fe²⁺-cit and FeCl₂.

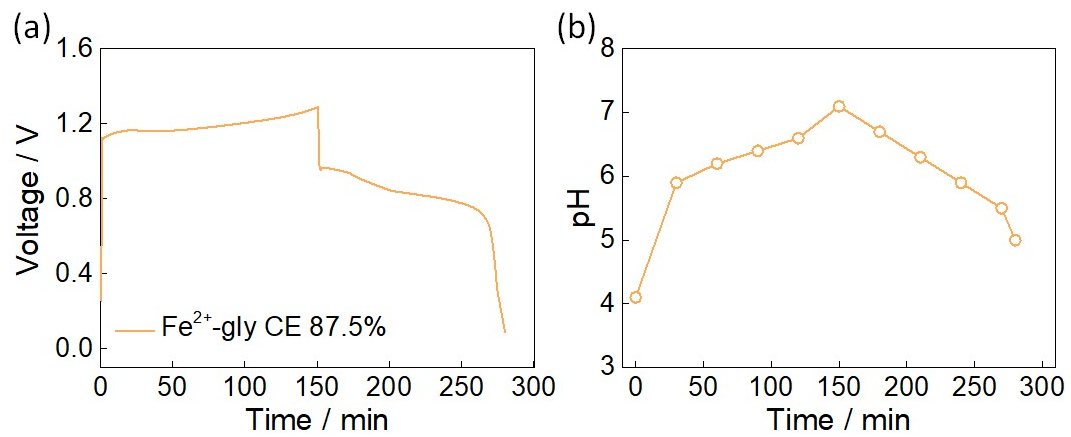


Fig. S4. (a) A complete charge-discharge cycle of the full cell adopting Fe²⁺-gly anolyte; (b) the corresponding pH variation of the Fe²⁺-gly anolyte during charge-discharge cycle.

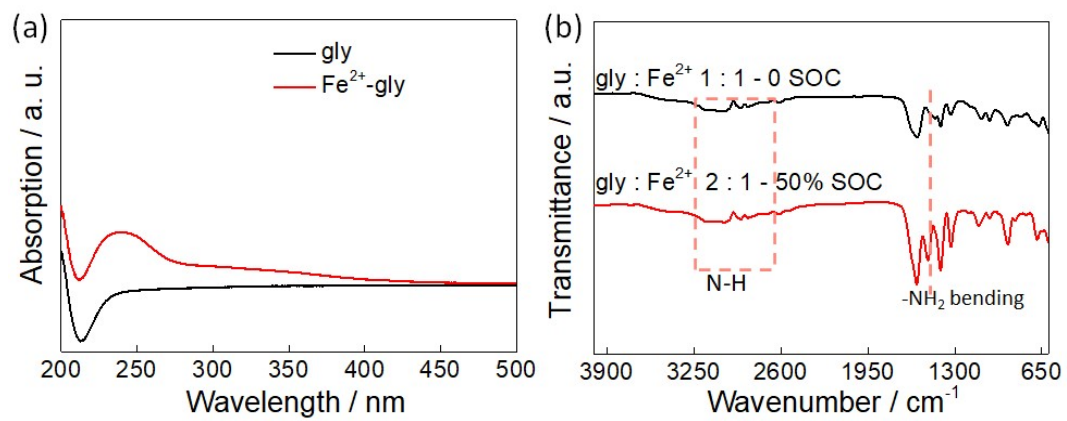


Fig. S5. (a) UV-vis spectrum of glycine and Fe²⁺-gly; (b) FTIR of Fe²⁺-gly at 0 and 50% SOC.

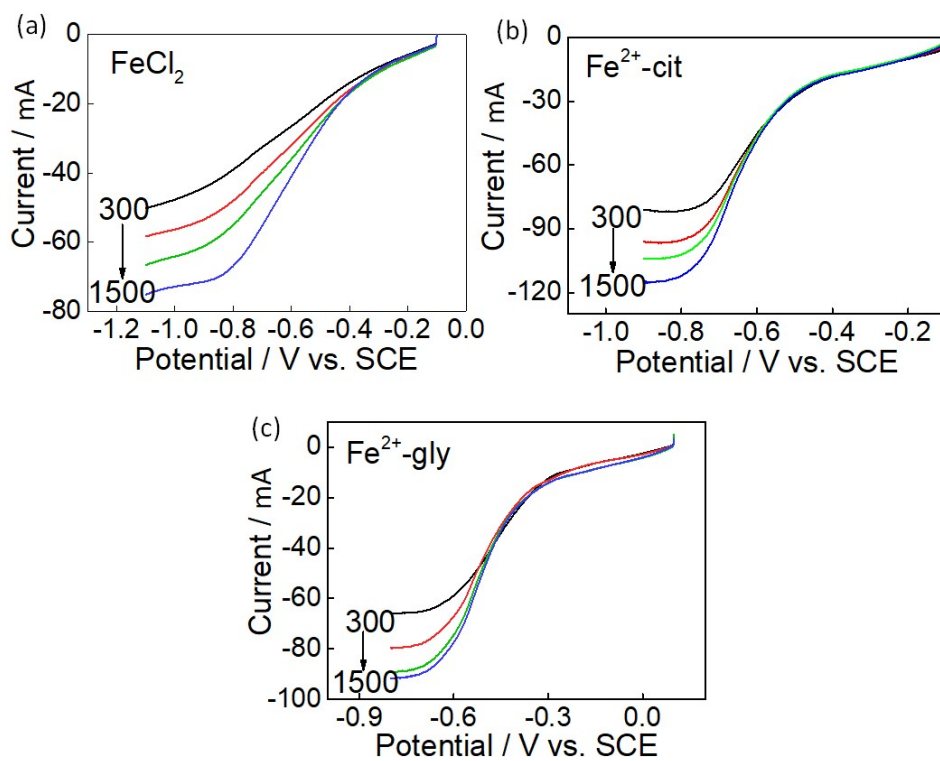


Fig. S6. RDE study of the reduction of (a) FeCl_2 (b) Fe^{2+} -cit and (c) Fe^{2+} -gly.

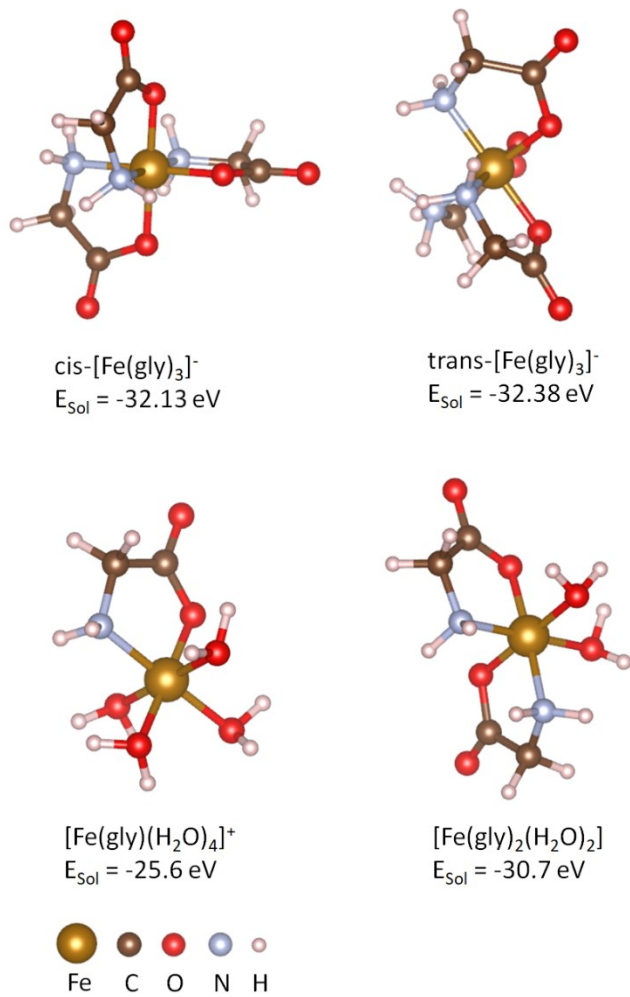


Fig. S7. The calculated solvation energy of various Fe^{2+} solvation structures.

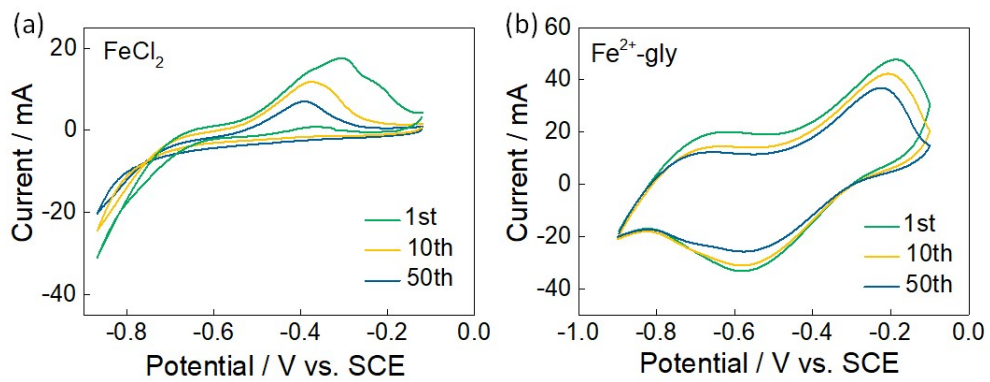


Fig. S8. The long-term CV test for (a) FeCl₂ and (b) Fe²⁺-gly at the scanning rate of 5 mV s⁻¹ vs. SCE.

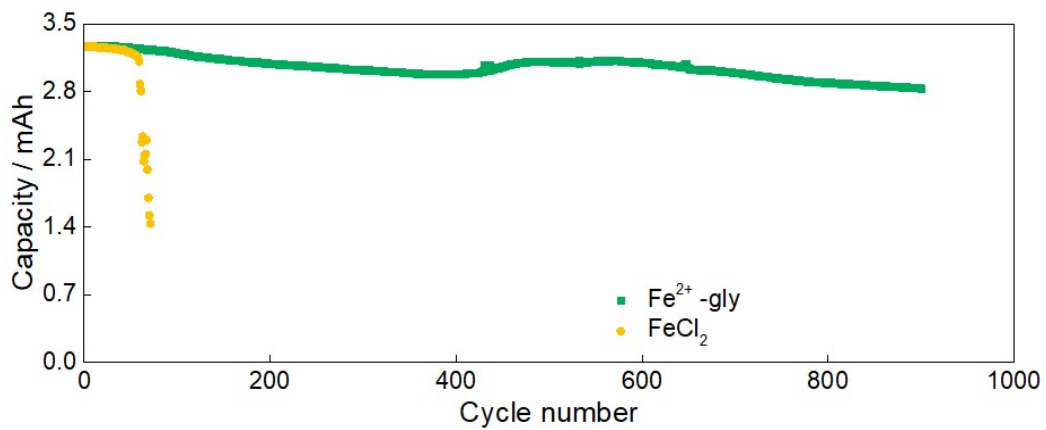


Fig. S9. The long-term stability tests of symmetrical cell using FeCl₂ and Fe²⁺-gly after 900 cycles.

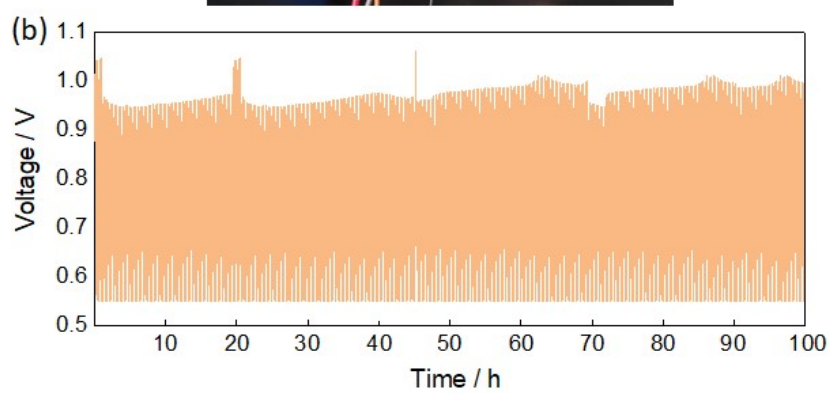
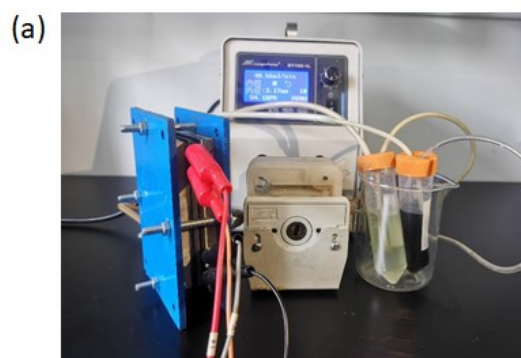


Fig. S10. (a) All-iron flow battery setup for charge-discharge tests and (b) voltage profiles.

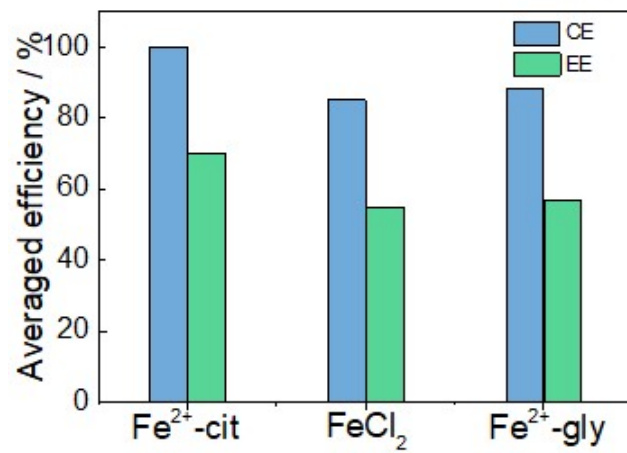


Fig. S11. The averaged CE and EE of full cell adopting different analytes.

4

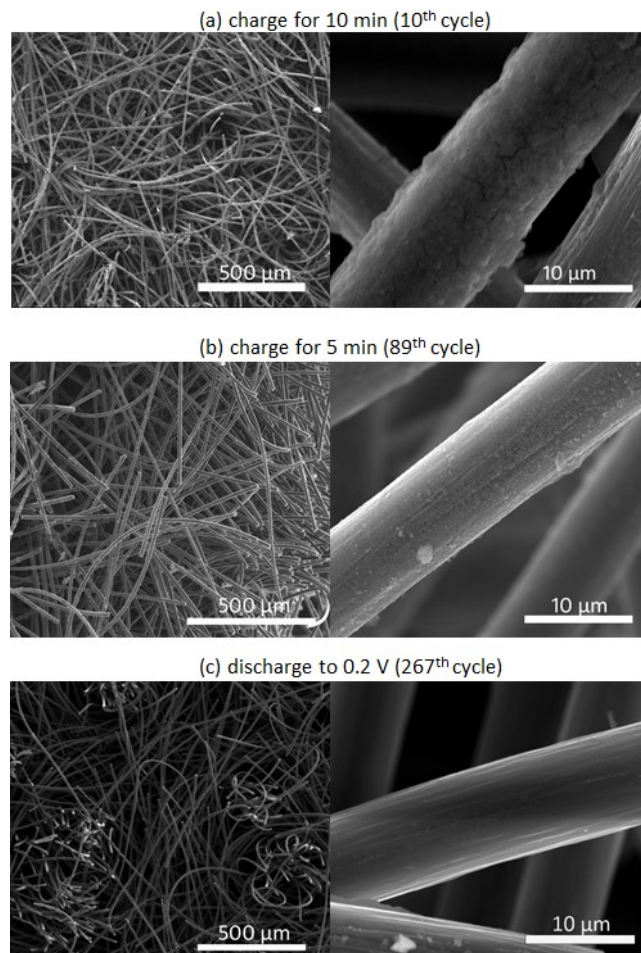


Fig. S12. The SEM morphologies of carbon felt in Fe^{2+} -cit anolyte at different charge/discharge states in different charge-discharge cycles.

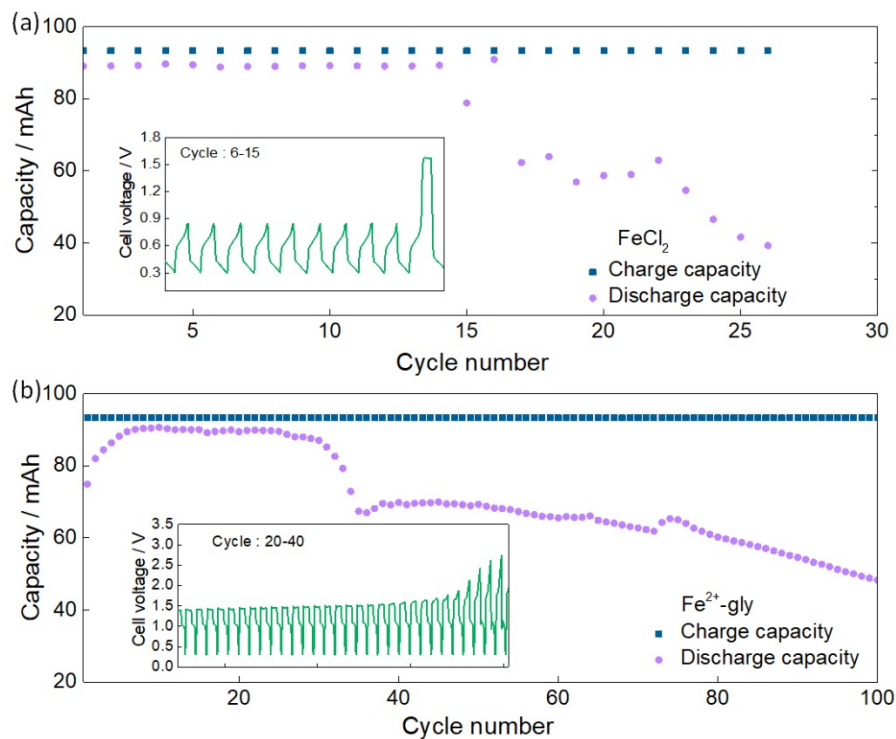


Fig. S13. The cycling performance and charge-discharge profile of the full cell adopting (a) FeCl₂ and (b) Fe²⁺-gly as anolyte at 20 mA cm⁻².

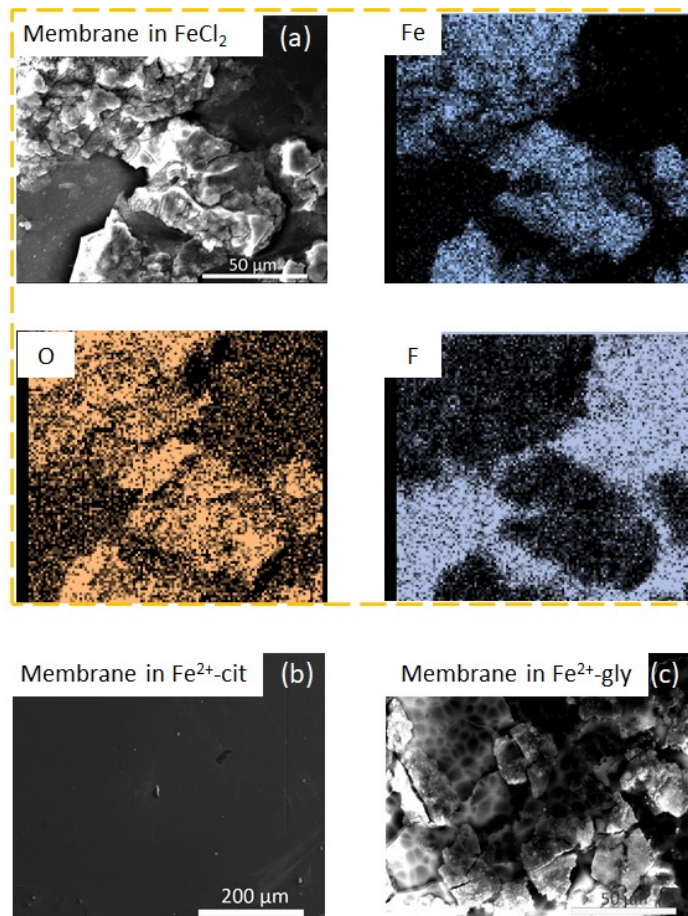


Fig. S14. The membrane morphology of the negative side cycled in different anolytes.

Note: the membranes in both FeCl₂ and Fe²⁺-gly anolytes were contaminated by iron oxides, whereas in Fe²⁺-cit the membrane was uncontaminated.

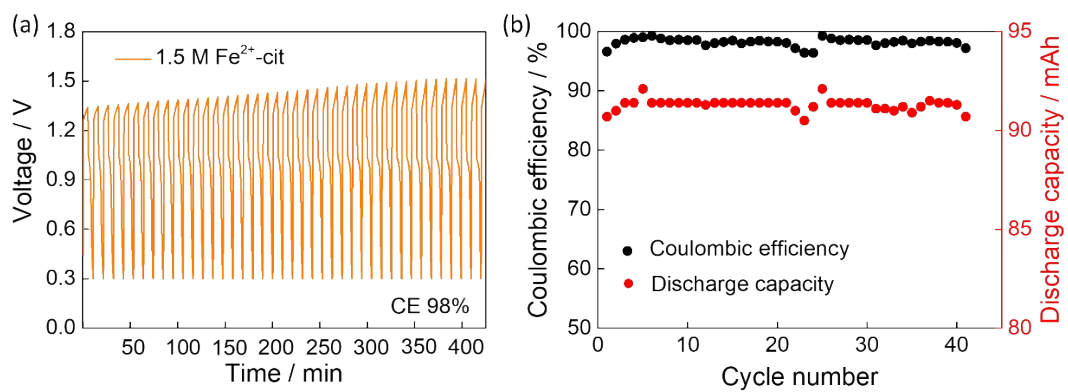


Fig. S15 The charge-discharge profiles and cycling performance of the flow cell adopting 1.5 M Fe²⁺-cit.

Table S1. Diffusion constants obtained by Levich plot

Composition	Diffusion constant / $\text{cm}^2 \text{s}^{-1}$
10 mM FeCl_2	2.3×10^{-8}
10 mM FeCl_2 + 10 mM citrate	5.2×10^{-8}
10 mM FeCl_2 + 10 mM glycine	3.7×10^{-8}

Table S2. Comparison with other all-iron RFBs

Raw material	FeCl ₂ /FeCl ₂ +Ch Cl+EG [22]	Fe ₃ O ₄ /Fe(CN) ₆ ⁴⁻ [23]	Fe(acac) ₃ / Fe ²⁺ [24]	Fc1N112-TFSI / Fe(acac) ₃ [25]	Fe(DIPSO) / Fe(CN) ₆ ⁴⁻ [26]	[Fe(TEOA)OH] ⁻ / Fe(CN) ₆ ⁴⁻ [34]	[Fe(cit) ₂] ⁶⁻ / Fe ²⁺
Cost / \$ kg ⁻¹	23	22	652	535	200	42	19
Anode capacity / Ah L ⁻¹	69.7	5.4	13.4	2.7	2.7	5.4	80 ^{**}
Cycle life	16 [*]	150	100	100	25	110	300

Note *: The data was obtained the charge-discharge cycles utilizing 0.5:1:4 FeCl₂:ChCl:EG.

** : The data was the available capacity corresponding to the [Fe(cit)₂]⁶⁻ maximum solubility of 1.5 M.